Substituent Effects on the Self-Assembly/Coassembly and Hydrogelation of Phenylalanine Derivatives

*Wathsala Liyanage and Bradley L. Nilsson**

Department of Chemistry, University of Rochester, Rochester, NY, 14627-0216, USA.

E-mail: nilsson@chem.rochester.edu

Fax: +1 585 276-0205; Tel. +1 585 276-3053

Supporting Information

Experimental Section

Materials.

Commercially available Fmoc amino acids and solvents were used without further purification except where noted. Water for gelation experiments was purified using a nanopure filtration system (Barnstead, NANOpure DIamond 0.2 mm filter, 18 W).

Assembly and Hydrogelation.

Fmoc-Phe derivatives were dissolved in dimethyl sulfoxide (DMSO, Aldrich) at concentrations of 247 mM. The DMSO stock solutions were then diluted into unbuffered water to a final amino acid concentration of 4.9 mM in 2% DMSO/H2O (v/v). These suspensions were gently mixed with a pipettor after which the suspensions were allowed to stand at room temperature; for Fmoc-Phe derivatives that effectively self-assemble, the initial opaque suspension spontaneously transformed into an optically transparent hydrogel as a function of time. Fmoc-Phe derivatives that do not effectively self-assemble were instead observed to precipitate from solution. Coassembly experiments were conducted by mixing 247 mM DMSO stock solutions of each Fmoc-Phe derivative in equimolar ratios. The coassembly mixtures were then diluted into unbuffered water to a final concentration of 4.9 mM total amino acid in 2% DMSO/H2O (v/v). Following dilution, each sample was allowed to stand at room temperature as described above.

Circular Dichroism (CD) Spectroscopy.

CD spectra were recorded on an AVIV 202 circular dichroism spectrometer. Coassembly mixtures were prepared by mixing DMSO solutions of each Fmoc-Phe derivative (247 mM) in 1:1 ratios prior to dilution with unbuffered water to final concentrations of 4.94 mM Fmoc amino

acid in 2% DMSO/H2O (v/v). The solutions were immediately transferred to a 0.1 mm path length quartz cuvette (Hellma), and gelation was allowed to proceed in the cuvette. Spectra were obtained from 350 to 190 nm with a 1.0 nm step, 1.0 nm bandwidth, and 6 s collection time per step at 25 ºC. The AVIV software was used for background subtraction and data smoothing with a least-squares fit.

Transmission Electron Microscopy (TEM)

Gel samples (10 mL) were applied directly onto 200 mesh carbon-coated copper grids and allowed to stand for 1 min. Excess gel was carefully removed by capillary action (using filter paper) and the grids were stained with a saturated solution of freshly filtered uranyl acetate (10 mL for 2 min). Excess stain was removed by capillary action and the grids were allowed to air-dry for 10–15 min. Fibril were imaged using a Hitachi 7650 transmission electron microscope with an accelerating voltage of 80 kV. Digital images were captured using an attached 11 megapixel Gatan Erlangshen digital camera system. Fibril dimensions were measured using ImageJ64 software (http://rsbweb.nih.gov/ij/); fibril dimensions were reported as the average of at least 100 measurements of unique fibrils with error as the standard deviation about the mean.

Scanning Electron Microscopy (SEM)

Samples were air-dried onto a round cover glass, mounted onto an aluminium stub and sputter coated (2 min) with gold at 1Å s-1 using a low vacuum sputter coating system (DENTON VACUUM Desk II) at 100 mTorr pressure in 15 mA current to achieve conformal conductive coating on the samples. Images were taken using a Zeiss Aurgia Supra40-VP field emission scanning microscope in backscatter electron detector mode with an accelerating voltage of 5 kV.

Rheology

Rheological measurements were conducted on a Discovery HR-2 hybrid rheometer operating in oscillatory mode using a 20 mm parallel plate geometry equipped with a solvent trap filled with silicone oil to prevent sample evaporation. DMSO stock solutions of Fmoc-Phe derivatives were diluted into water (4.9 mM total amino acid, 2% DMSO/H2O (v/v)) as described previously and immediately applied to the Peltier plate. Dynamic time sweep experiments were immediately performed at 25 ºC over 30–60 min with an angular frequency of 6.283 rad s-1 and 0.2% strain. Dynamic frequency sweep experiments were then performed from 0.1–100 rad s-1 at 0.2% strain at 25 ºC. Measurements were performed in the linear viscoelastic region of each gel as determined by prior strain sweep experiments. The reported values for storage modulus (G′) and loss modulus (G²) are an average of at least three experiments on unique hydrogel samples with the error reported as the standard deviation about the mean.

Calculation of Charge Density Maps and Electrostatic Potentials

Electrostatic potentials were computed using Hartree-Fock with the 6-31G* basis set with a scale of -100 to +100 kJ mol-1 (Spartan, Wave Function Inc.). Molecular volumes and bond polarization were calculated for energy-minimized para X-toluene as an approximation of the benzyl side chain of the Fmoc-para-X-Phe amino acids.

Single Crystal X-ray Structure Determination of Fmoc-4-CH3-Phe Crystals

Data collection. An Fmoc-4-CH3-Phe crystal (0.45 × 0.14 × 0.12 mm^3) (obtained by the spontaneous transition of hydrogel fibrils to crystals) was placed onto the tip of a 0.1 mm

diameter glass capillary tube or fiber and mounted on a Brüker SMART APEXII CCD platform diffractometer for a data collection at 100.0(5) K (APEX2, version 2013.2-0; Brüker AXS: Madison, WI, 2013). A preliminary set of cell constants and an orientation matrix were calculated from reflections harvested from three orthogonal wedges of reciprocal space. The full data collection was carried out using MoKa radiation (graphite monochromator) with a frame time of 60 seconds and a detector distance of 4.01 cm. A randomly oriented region of reciprocal space was surveyed: four major sections of frames were collected with 0.50º steps in w at four different f settings and a detector position of -38º in 2q. The intensity data were corrected for absorption (Sheldrick, G. M. SADABS, version 2008/1; University of Göttingen: Göttingen, Germany, 2008). Final cell constants were calculated from the xyz centroids of 4007 strong reflections from the actual data collection after integration (SAINT, version 7.68A; Bruker AXS: Madison, WI, 2009). Supporting Information, Appendix 1 contains a detailed presentation of the crystallographic data.

Structure solution and refinement. The structure was solved using SIR97 (Altomare, A.; Burla, M. C.; Camalli, M.; Cascarano, G. L.; Giacovazzo, C.; Guagliardi, A.; Moliterni, A. G. G.; Polidori, G.; Spagna, R. SIR97: A new program for solving and refining crystal structures; Istituto di Cristallografia, CNR: Bari, Italy, 1999) and refined using SHELXL-2013. The space group P212121 was determined based on systematic absence. A direct-methods solution was calculated which provided most non-hydrogen atoms from the E-map. Full matrix least square/difference Fourier cycles were performed which located the remaining non-hydrogen atoms. All non-hydrogen atoms were refined with anisotropic displacement parameters. The positional parameters for all hydrogen atoms except for those of the methyl group were found from the difference Fourier map and refined freely. The hydrogen atoms of the methyl group

were placed and refined geometrically. All hydrogen atoms were refined relatively to isotropic displacement parameters. The final full matrix least squares refinement converged to R1 = 0.0544(F2, I>2σ (I)) and wR2 = 0.1260 (F2, all data). Unless noted otherwise all structural diagrams containing thermal displacement ellipsoids are drawn at the 50 % probability level.

Single Crystal X-ray Structure Determination of Fmoc-4-CN-Phe/Fmoc-4-NO2-Phe Cocrystals

Data collection. An Fmoc-4-CN-Phe/Fmoc-4-NO2-Phe cocrystal (0.28 × 0.08 × 0.04 mm^3) (obtained by the spontaneous transition of hydrogel fibrils to crystals) was placed onto the tip of a 0.1 mm diameter glass capillary tube or fiber and mounted on a Brüker SMART APEX II CCD Platform diffractometer for a data collection at 100.0(5) K (APEX2, version 2013.2-0; Brüker AXS: Madison, WI, 2013). A preliminary set of cell constants and an orientation matrix were calculated from reflections harvested from three orthogonal wedges of reciprocal space. The full data collection was carried out using MoKα radiation (graphite monochromator) with a frame time of 120 seconds and a detector distance of 4.01 cm. A randomly oriented region of reciprocal space was surveyed: four major sections of frames were collected with 0.50º steps in w at four different ϕ settings and a detector position of -38º in 2θ. The intensity data were corrected for absorption (Sheldrick, G. M. SADABS, version 2012/1; University of Göttingen: Göttingen, Germany, 2012). Final cell constants were calculated from the xyz centroids of 1306 strong reflections from the actual data collection after integration (SAINT, version 8.27B; Brüker AXS: Madison, WI, 2013). Supporting Information, Appendix 2 contains a detailed presentation of the crystallographic data.

Structure solution and refinement. The structure was solved using SIR97 (Altomare, A.; Burla, M. C.; Camalli, M.; Cascarano, G. L.; Giacovazzo, C.; Guagliardi, A.; Moliterni, A. G. G.; Polidori, G.; Spagna, R. SIR97: A new program for solving and refining crystal structures; Istituto di Cristallografia, CNR: Bari, Italy, 1999) and refined using SHELXL-97 (Sheldrick, G. M. SHELXL-2013/2 University of Göttingen: Göttingen, Germany, 2013). The space group P212121 was determined based on systematic absences. A direct-methods solution was calculated which provided most non-hydrogen atoms from the E-map. Full-matrix least squares/difference Fourier cycles were performed which located the remaining non-hydrogen atoms. All non-hydrogen atoms were refined with anisotropic displacement parameters. All hydrogen atoms were placed in ideal positions and refined as riding atoms with relative isotropic displacement parameters. Due to the lack of significant anomalous dispersion effects, the correct enantiomer was assigned and all Friedel opposites were merged in the final refinement. The final full matrix least squares refinement converged to R1 = 0.0601 (F2, I > 2s(I)) and wR2 = 0.1428 (F2, all data). Unless noted otherwise all structural diagrams containing thermal displacement ellipsoids are drawn at the 50 % probability level.

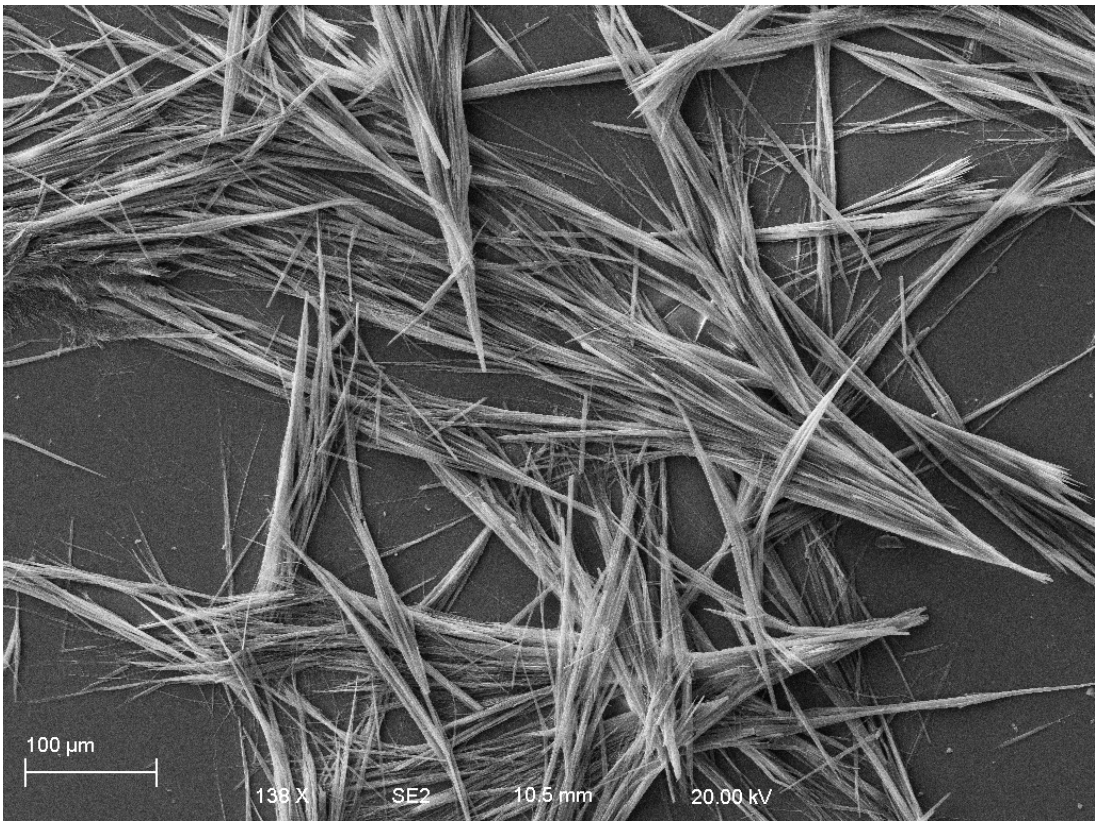

Figure S1.SEM image of Fmoc-4-CH_3-Phe crystals formed by spontaneous transition from self-assembled hydrogels (138× magnification).

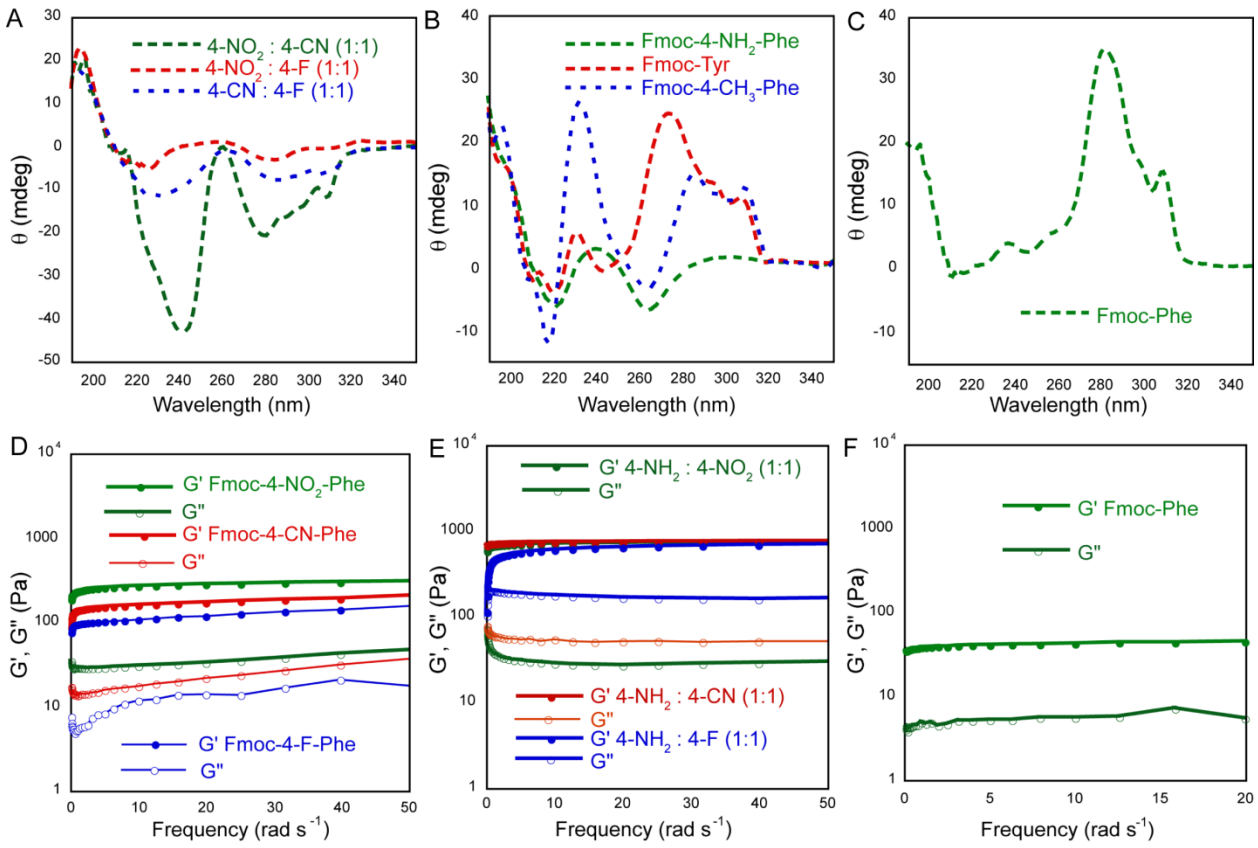

Figure S2.A-C. CD spectra of hydrogels for each Fmoc-Phe derivative. A. Electron deficient Fmoc-Phe derivatives; B. Electron rich Fmoc-Phe derivatives; C. Fmoc-Phe. D-F. Viscoelasticity of assembled hydrogels as determined by measurement of storage (G′) and loss (G″) moduli by oscillatory rheology dynamic frequency sweep experiments (4.9 mM Fmoc-4-X-Phe derivative). D. Electron deficient Fmoc-Phe derivatives; E. Electron rich Fmoc-Phe derivatives; F. Fmoc-Phe.

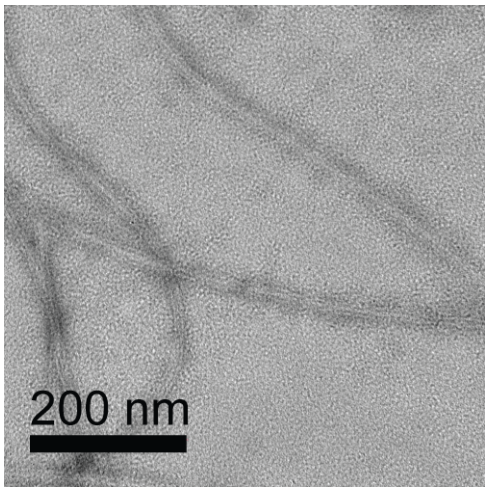

Figure S3.TEM image of Fmoc-Phe/Fmoc-Tyr cofibrils formed after 1 week of incubation.

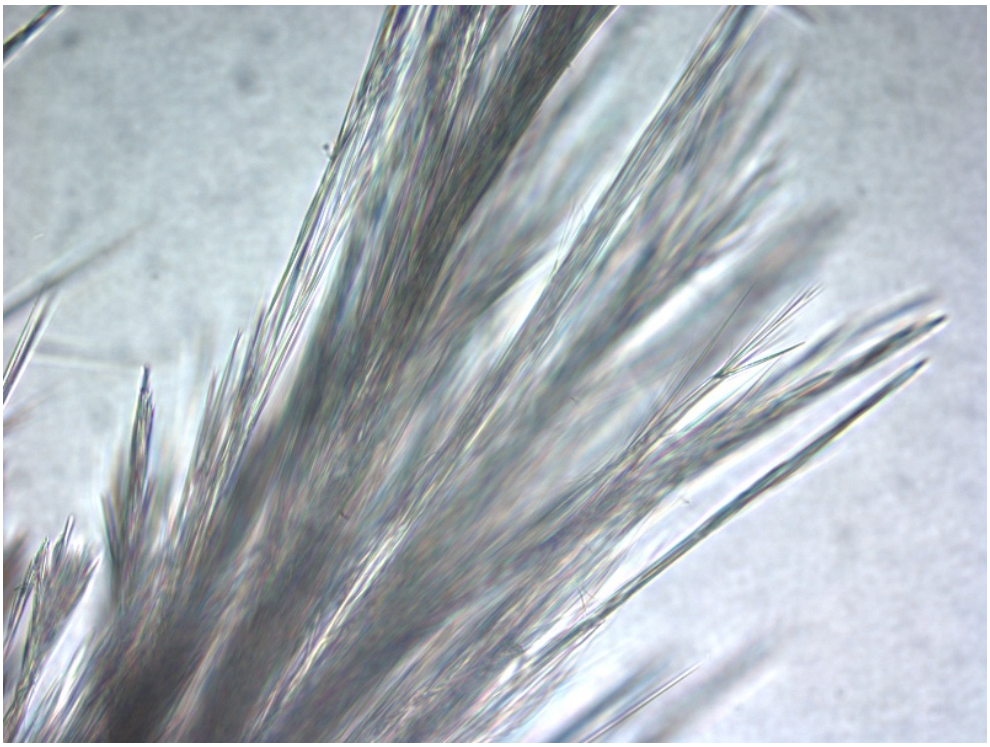

Figure S4. Photomicrograph of Fmoc-4-CH_3-Phe/Fmoc-Phe (1:1) cocrystals formed by spontaneous transition from hydrogel fibrils (4.9 mM amino acid in 2% DMSO in H_2O) (40×magnification).

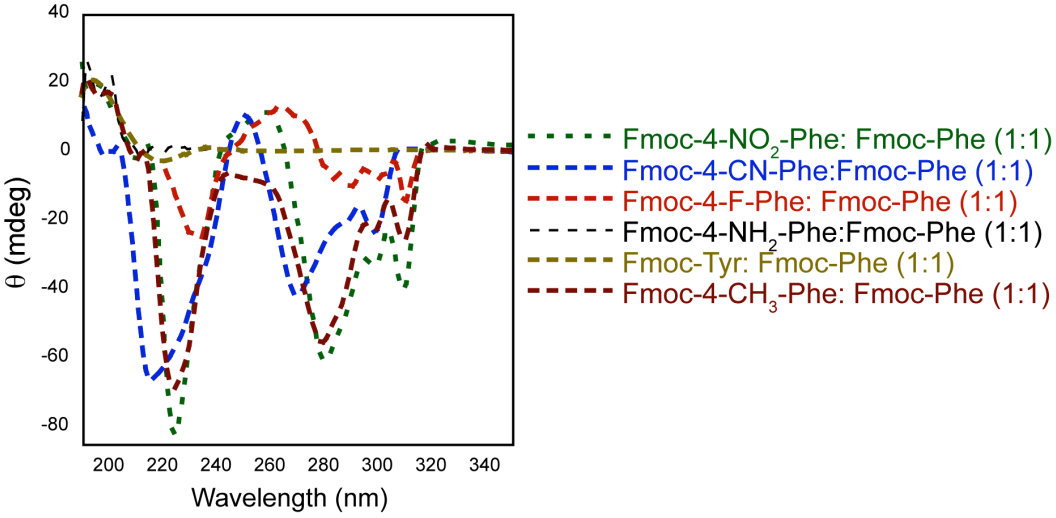

Figure S5. CD spectra of 4.9 mM coassembled mixtures of Fmoc-4X-Phe/Fmoc-Phe variants.

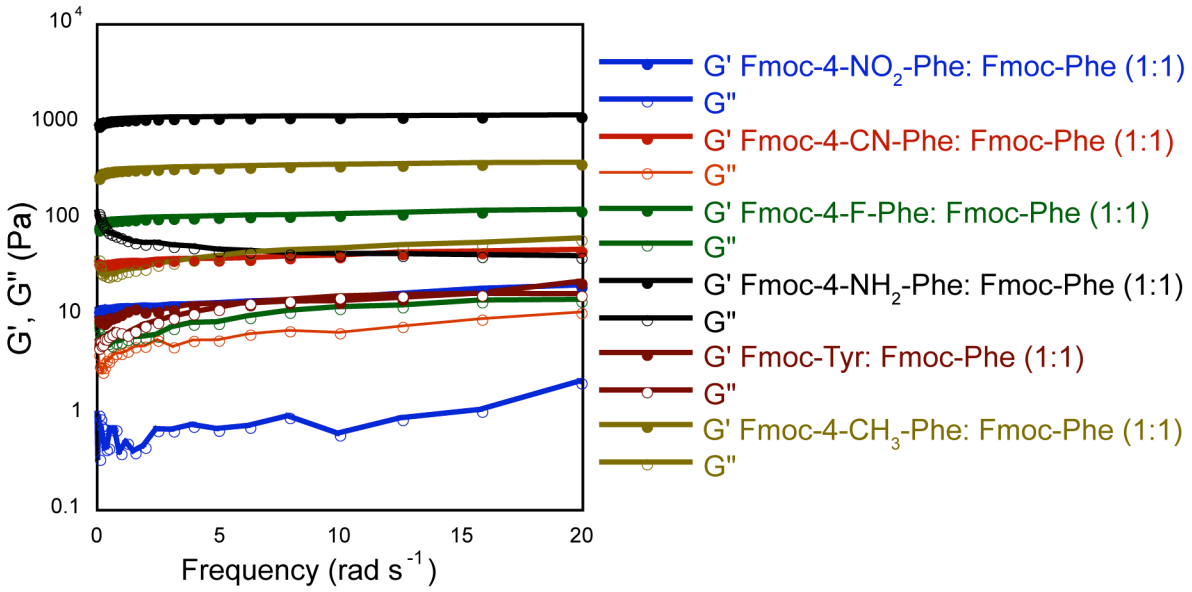

Figure S6. Dynamic frequency sweep of 4.9 mM Fmoc-4-X-Phe/Fmoc-Phe coassembly mixtures.

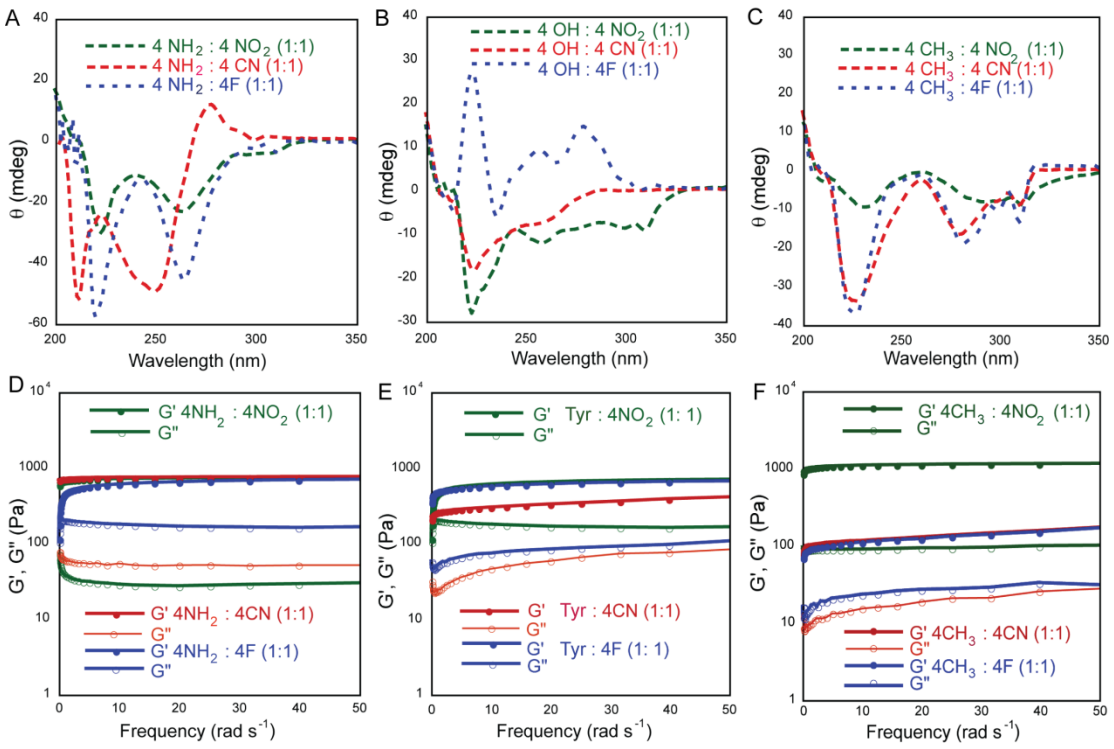

Figure S7.A-C.CD spectra for coassembled electron-rich/electron-deficient Fmoc-4-X-Phe pairs. D-F. Rheological viscoelasticity for coassembled electron-rich/electron-deficient Fmoc-4-X-Phe pairs as determined by dynamic frequency sweep experiments (4.9 mM total Fmoc-4-X-Phe).

Figure S8.A photomicrograph (40× magnification) of Fmoc-4-NO2-Phe/Fmoc-4CN-Phe (1:1) co crystal microtubes spontaneously formed from hydrogel fibrils 3 days in 2% DMSO in H_2O.

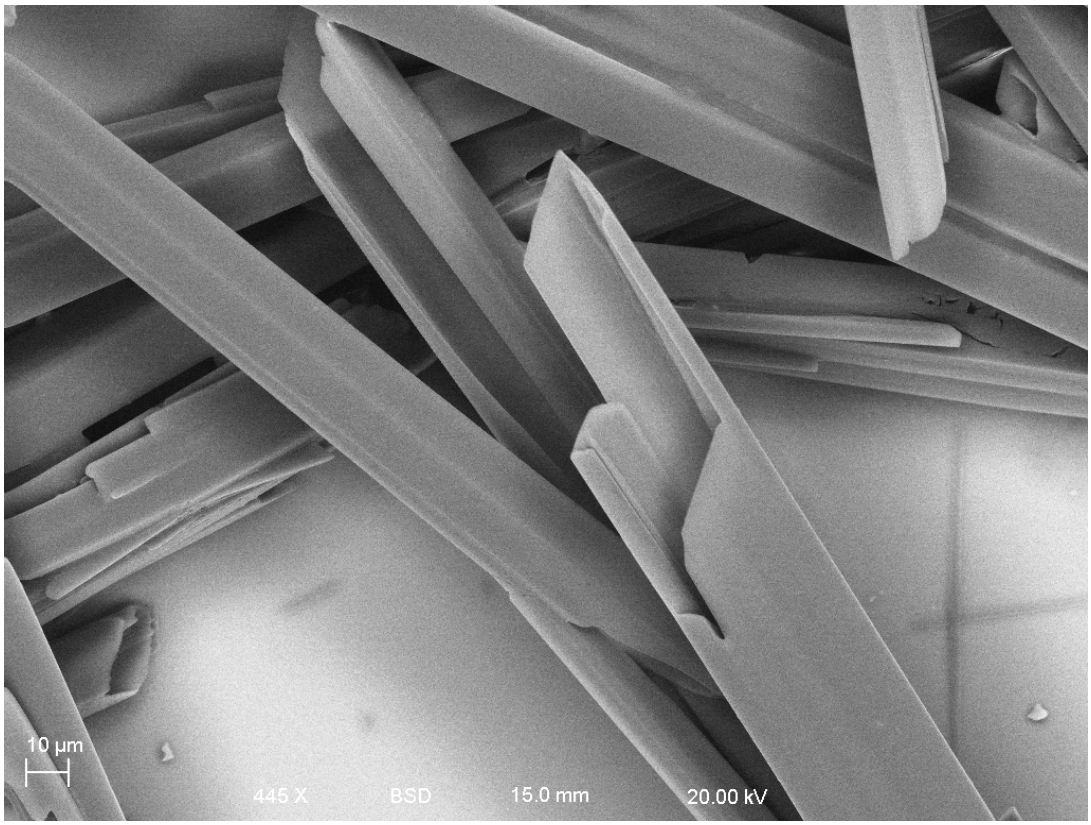

Figure S9. SEM image of Fmoc-4-NO2-Phe/Fmoc-4-CN-Phe (1:1) cocrystal microtubes spontaneously formed from hydrogel fibrils (445× magnification).

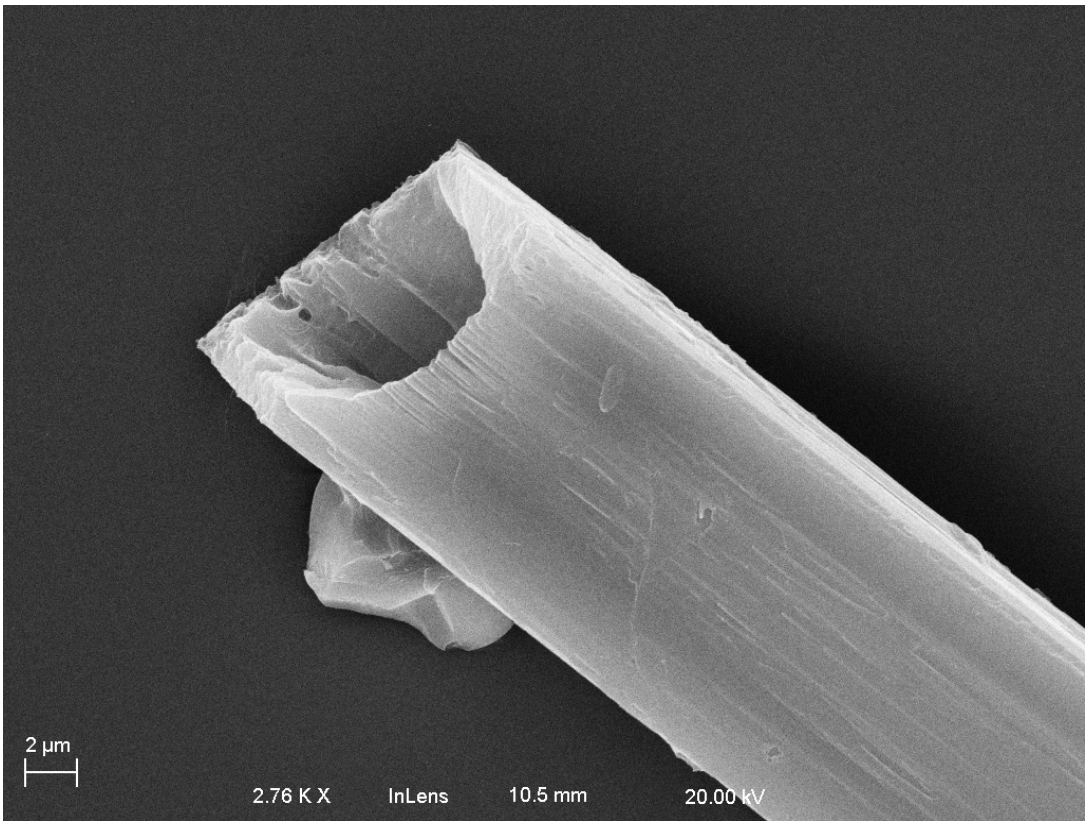

Figure S10. SEM image of Fmoc-4-NO2-Phe/Fmoc-4-CN-Phe (1:1) cocrystals formed spontaneously from hydrogel fibrils (2720× magnification).

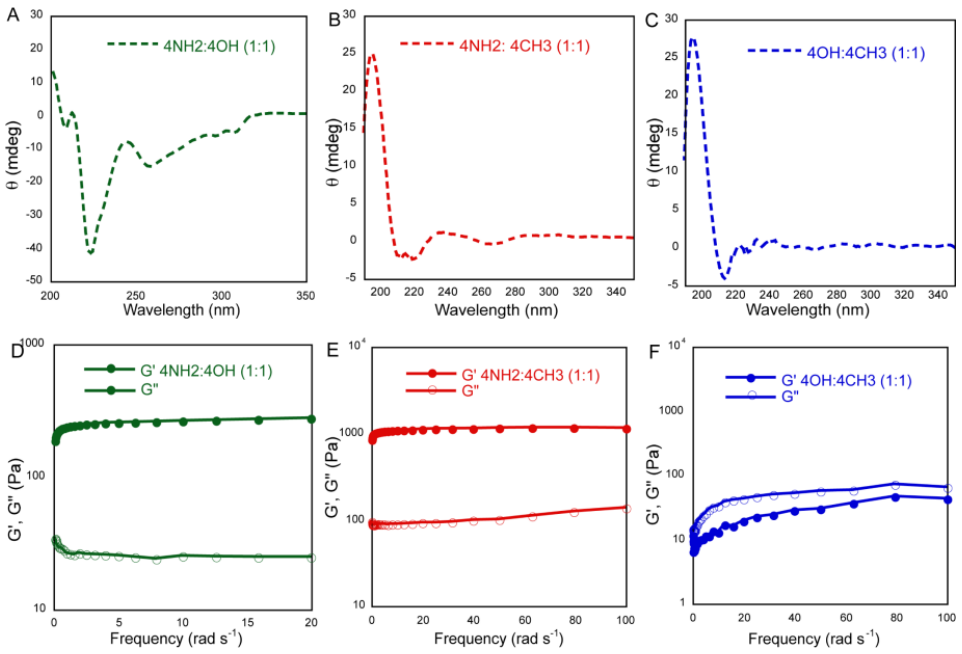

Figure S11. A-C. CD spectra of electron-rich/electron-rich coassembled pairs of Fmoc-4-X-Phe hydrogels. D-F. Oscillatory rheology dynamic frequency sweep characterization of electron-rich/electron-rich coassembled pairs of Fmoc-4-X-Phe hydrogels(4.9 mM total Fmoc-4-X-Phe).

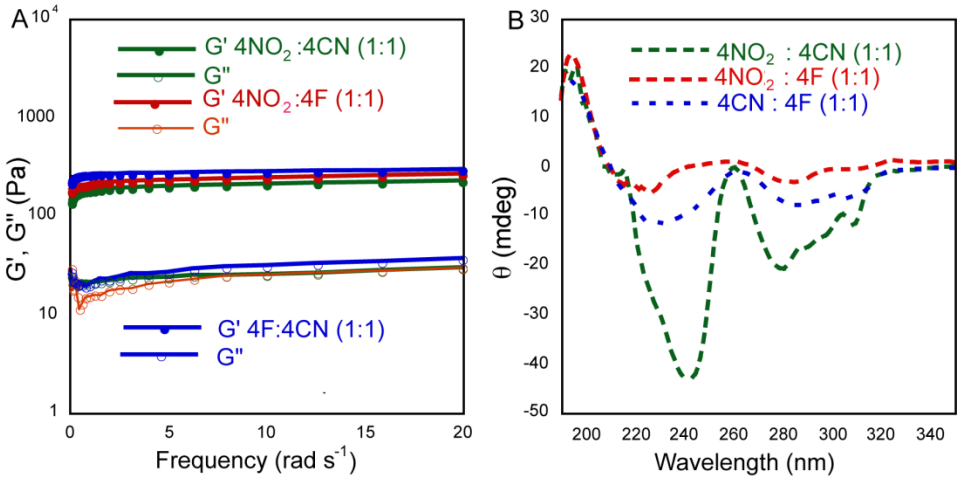

Figure S12. A. Oscillatory rheology dynamic frequency sweep characterization of electron-deficient/electron-deficient coassembled pairs of Fmoc-4-X-Phe hydrogels(4.9 mM total Fmoc-4-X-Phe). B. CD spectra of electron-deficient/electron-deficient coassembled pairs of Fmoc-4-X-Phe hydrogels.

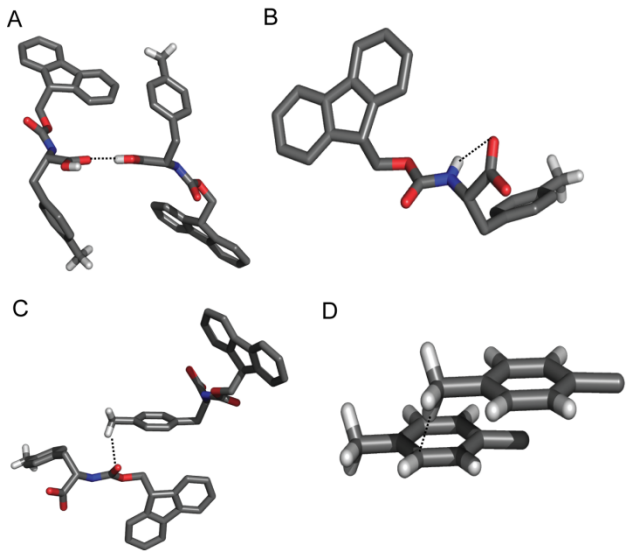

Figure S13. Intermolecular interactions between adjacent Fmoc-4-CH_3-Phe monomers in crystal structure: A. Moderately strong hydrogen bonds (OH···O), B. weak hydrogen bonds (NH···O) within the strand (intramolecular interaction), C. Non-conventional hydrogen bonds (CH···O), D. Interaction between the methyl C-H and *ortho* C-H on adjacent benzyl rings.

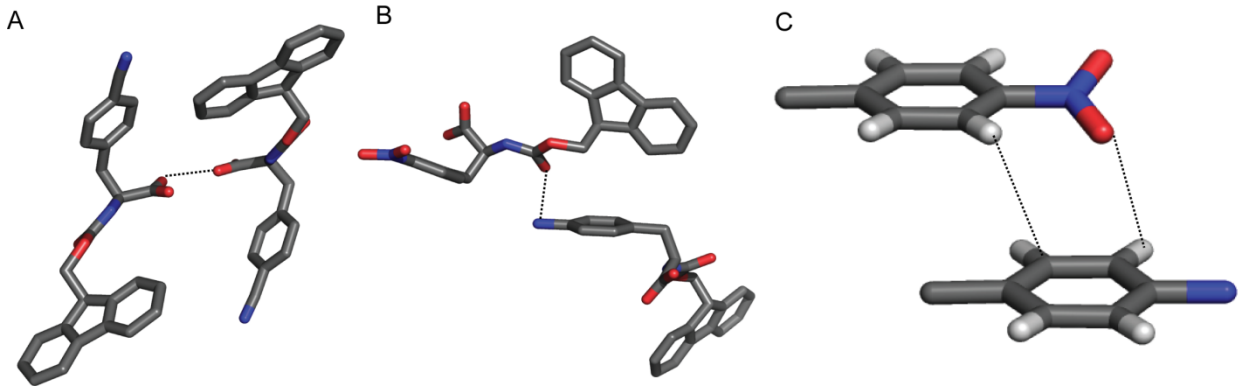

Figure S14. Intermolecular interactions between Fmoc-4-NO_2-Phe/Fmoc-4-CN-Phe monomers in crystal structure: A. Moderately strong hydrogen bonds (OH···O), B. Moderately strong intermolecular electrostatic interactions (O_2N [δ+]···[δ-] O=C)., C. Local dipole interactions.